processes

MDPI

Article

Study on the Extraction Mechanism of Metal Ions on Small Molecular Phase of Tar-Rich Coal under Ultrasonic Loading

Zetang Wang [1,2], Yuan Bao [3,*], Chaoyong Wang [1,2] and Yiliang Hu [3]

[1] Key Laboratory of Coalbed Methane Resources and Reservoir Formation Process, Ministry of Education, China University of Mining and Technology, Xuzhou 221008, China; wangzetang@cumt.edu.cn (Z.W.); wangcy@cumt.edu.cn (C.W.)
[2] School of Resources and Geosciences, China University of Mining and Technology, Xuzhou 221008, China
[3] College of Geology and Environment, Xi'an University of Science and Technology, Xi'an 710054, China; huyl1130@foxmail.com
* Correspondence: y.bao@foxmail.com

Abstract: This study aims to elucidate the mechanism by which the ultrasonic loading of metal affects the extraction of small molecular phase substances (low molecular compounds) in tar-rich coal. Tar-rich coal samples were collected from the Huangling mining area in the southeastern Ordos Basin, China. The coal, the leaching solution of the coal, the extraction products, and the extraction residual coal samples with different metal ions loaded by ultrasound were analyzed using field emission scanning electron microscopy, pH detection, gas chromatography–mass spectrometry, a Fourier transform infrared spectrometer, and an X-ray diffractometer. The obtained results indicated that the ultrasonic loading of coal samples with different metal ions (Mn^{2+}, Co^{2+}, Cu^{2+}, Fe^{2+}, and Ni^{2+}) promoted the extraction of small molecular phase substances in coal and increased the proportion of extracted aliphatic hydrocarbons, alkylbenzene, naphthalene, phenanthrene, and other compounds. The extraction rate of Mn^{2+} was the highest. Compared with the control group, the extraction rate was increased by 212%. After the ultrasonic loading of metal ions, the physical structure of the coal was loose and the contact area of the solvent increased; the degree of branching and the hydrogen enrichment of the residual coal decreased, the aromaticity increased, the interlayer spacing and stacking layers decreased, and the stacking degree and ductility increased. Metal ions exchanged with hydrogen ions in the coal molecules. At the same time, the metal ions were adsorbed in the coal molecules and effectively combined with free electrons in the coal molecules to catalyze; thus, the extraction effect of the small molecular phase of tar-rich coal was improved. This provides a new method for the clean and efficient utilization of tar-rich coal.

Keywords: tar-rich coal; metal ions; organic small molecule phase; solvent extraction; action mechanism

Citation: Wang, Z.; Bao, Y.; Wang, C.; Hu, Y. Study on the Extraction Mechanism of Metal Ions on Small Molecular Phase of Tar-Rich Coal under Ultrasonic Loading. *Processes* **2024**, *12*, 104. https://doi.org/10.3390/pr12010104

Academic Editors: Junjian Zhang and Zhenzhi Wang

Received: 28 November 2023
Revised: 25 December 2023
Accepted: 27 December 2023
Published: 1 January 2024

1. Introduction

Tar-rich coal refers to the use of low-temperature pyrolysis technology to extract coal tar; the tar yield is greater than 7% in the Gray-King assay of coal [1]. The tar-rich coal is a vast reserve of coal-based oil and gas resources, with the oil resources contained in the tar-rich coal in Shaanxi Province alone ranking ninth in the world and equaling 3.58 times that of China's confirmed petroleum resources and 1.57 times that of the United States [2]. As a coal resource that combines oil and gas, tar-rich coal has already attracted preliminary attention from scholars in various regions, and extensive research has been conducted specifically on its most important coal tar resources [3,4]. The use of low-temperature pyrolysis technology to extract coal tar from it is associated with relatively high energy consumption and significant environmental pollution [5]. According to the two-phase structure model, coal consists of a covalently bonded large molecular network (host) and a mobile phase (guest). The mobile phase refers to the small molecular compounds that are trapped within the network [6–8]. Under mild extraction conditions, the small molecular

phase embedded within the large molecular network can be effectively separated using organic solvents, and the small molecular phase often consists of the "low-molecular-weight compounds" found in coal [9–11]. Many of these small molecular phase compounds can serve as high-quality chemical raw materials, which can be used in the production of various high-value basic materials or new chemical materials [12,13]. The tar-rich coal generally belongs to low- to medium-rank coal and is characterized by a low degree of coalification, which contains a significant amount of "low-molecular-weight compounds". Therefore, it provides a new method for the efficient and clean utilization of tar-rich coal [14,15].

Previous researchers conducted extensive studies on solvent extraction [9,16,17], and some of these solvents exhibited excellent dissolving effects, particularly with bituminous coal [18–24]. The main methods of extraction have also evolved into three categories: direct, indirect, and auxiliary [25–27]. Auxiliary extraction refers to the artificial interventions made during the original direct extraction process to increase product yield, such as heating, ultrasonics, microwaves, and so on [28–31]. In the past decade, thermal dissolution processes have also been developed to enhance the extraction of organic matter and produce hyper-coals [32]. Metal chloride is commonly employed as a catalyst due to its evident catalytic activity, which effectively enhances the thermal dissolution efficiency of coal and alters the composition of the resulting product when introduced [3,33]. For tar-rich coal with abundant small molecular compounds, low-temperature solvent extraction is a practical and efficient way to provide clean utilization. It also avoids the breaking of covalent bonds, making it an effective method for studying the macro-molecular structure of coal [26,34]. However, the low efficiency of conventional coal extraction methods is a major obstacle to the further advancement of this approach. Therefore, the research focus lies in effectively enhancing the extraction efficiency of small molecular phases in coal and optimizing the types and proportions of available organic matter compounds. In order to achieve this, our study specifically investigates tar-rich coal from the Huangling mining area in the southeastern part of the Ordos Basin. Under ultrasonic conditions, metal ions are loaded onto coal samples treated with ash removal by impregnation. Different coal samples loaded with metal ions through ultrasonication are subjected to Soxhlet extraction. The impact of the ultrasonic loading of different metal ions on the extraction efficiency of small molecular phases and the compound composition in coal samples is analyzed using weighing methods and gas chromatography–mass spectrometry (GC-MS) testing. Simultaneously, a comparison is made between the changes in the surface functional groups and the lattice structure of residual coal after ultrasonic loading with different metal ions, and the differential characteristics in the coal chemical structure are analyzed. Finally, by combining the morphological features of coal after ultrasonic loading with different metal ions and the changes in the acidity and alkalinity of the leachate, the mechanism of the impact of the ultrasonic loading of metal ions on the extraction of small molecular phases in tar-rich coal is further explored.

2. Experiment and Methods

2.1. Ultrasonic Loading Experiment of Metal Ions

The Ordos Basin is rich in abundant tar-rich coal resources, with the Jurassic coal seams comprising the majority; these seams are primarily dominated by long-flame coal [35]. The tar yield generally ranges from 7% to 12%. The samples were collected from the Yan'an Formation No. 2 coal seam in the Huangling mining area of the Jurassic coalfield in the Ordos Basin. Based on the Gray-King assay of coal (GB/T 1314-2007) [36], the tar yield was determined to be 9.8%, indicating that it is a typical tar-rich coal. The industrial analysis and elemental analysis data for the coal samples are shown in Table 1.

Table 1. Industrial analysis and elemental analysis of coal samples (HL coal).

Proximate Analysis (w_t%)				Ultimate Analysis (w_t%, daf)					Gray-King Assay (%)		
M_{ad}	A_{ad}	V_{daf}	FC_{ad}	C_{daf}	H_{daf}	O_{daf}	N_{daf}	$S_{t,daf}$	Moisture content	Tar yield	Semi-coke yield
1.18	5.85	35.90	59.60	73.15	5.10	20.05	1.359	0.34	4.50	9.80	76.40

M_{ad}, moisture on air-dried basis (ad); A_{ad}, ash on air-dried basis (d); V_{daf}, volatile matter on dry ash-free basis (daf); FC_{ad}, fixed carbon on air-dried basis; w_t%, daf, the weight percentage of various elements on a dry ash-free basis.

By investigating the commonly employed catalytic ions in previous studies, we selected the following five metal ions (Ni^{2+}, Fe^{2+}, Co^{2+}, Cu^{2+}, and Mn^{2+}) in order to conduct experiments for a comparative analysis of their catalytic efficacy. The first step involves pulverizing and sieving the coal sample (HL-Coal) to a particle size of 120–200 mesh, followed by drying at 80 °C for 8 h. Subsequently, the coal sample is subjected to demineralization treatment using hydrofluoric acid (HF) and hydrochloric acid (HCl). The demineralization process is as follows: 20 g of pulverized coal sample is placed in a beaker. First, 120 mL of room temperature HCl (6 mol/L) is added, and the mixture is stirred for 24 h. After filtration, the coal sample is then subjected to another 24 h stirring at room temperature with HF (40 wt.%). After filtration, the coal sample is washed with deionized water until the solution becomes neutral. Following demineralization, the coal is dried at 80 °C for 8 h to obtain ash-free coal. Subsequently, 5 g of the ash-free coal sample is immersed in 100 mL of a $NiCl_2$ solution (1% concentration) with a coal-to-$NiCl_2$ ratio of 100:1. The mixture is subjected to ultrasonic agitation in a water bath for 6 h. The ultrasonic treatment device model used in this experiment is the KQ-500DE, with a power setting of 40% at a frequency of 40 kHz. After filtration and separation, the mixture is dried at 80 °C for 8 h, and the loaded coal sample containing Ni^{2+} and the corresponding leaching aqueous solution are obtained.

Using the same method, the ash-free coal samples are separately immersed in solutions of $FeCl_2$, $CoCl_2$, $CuCl_2$, and $MnCl_2$, each with a concentration of 1%. This results in the obtaining of ash-free coal samples loaded with Fe^{2+}, Co^{2+}, Cu^{2+}, and Mn^{2+} metal ions, along with their respective leaching aqueous solutions. Subsequently, the ash-free coal samples loaded with different metal ions are used in the subsequent organic matter extraction experiments (Soxhlet extraction method). For this experiment, there are three control groups: one consists of 5 g of ash-free coal and ultrapure water; the second involves ultrapure water with the addition of different metal ions; the third comprises only ultrapure water. All three groups undergo equivalent treatment involving water bath ultrasonic agitation. The metal ions used in the metal ion loading experiment are all in the form of metal chlorides, thus eliminating the influence of chloride ions and focusing solely on the effects of metal ion loading. The overall experimental approach is illustrated in Figure 1.

2.2. Acidity and Alkalinity (pH) Test

The pH levels of the leaching aqueous solutions, including those from all the blank groups, after the ultrasonic treatment of coal loaded with different metal ions, were determined using a pH meter. The pH meter used was a LeiCi PHS-3C, with a testing range of −2 to 18 pH units and a minimum resolution of 0.01 pH units. It is equipped with the combination electrode (E-201F), allowing for the precise and rapid measurement of the pH levels of solutions.

2.3. Scanning Electron Microscopy

The microstructures of the coal samples loaded with different metal ions under ultrasonic treatment were observed using a field emission scanning electron microscope (FE-SEM) with the model number JSM-7610F from Japan. The magnification range used was 25 to 1,000,000 times (120 × 90 mm). Additionally, a semi-immersion objective and a high-performance electron optical system were employed to provide stable and high spatial resolution for observation and analysis in an in situ position, following the method described by literature [37].

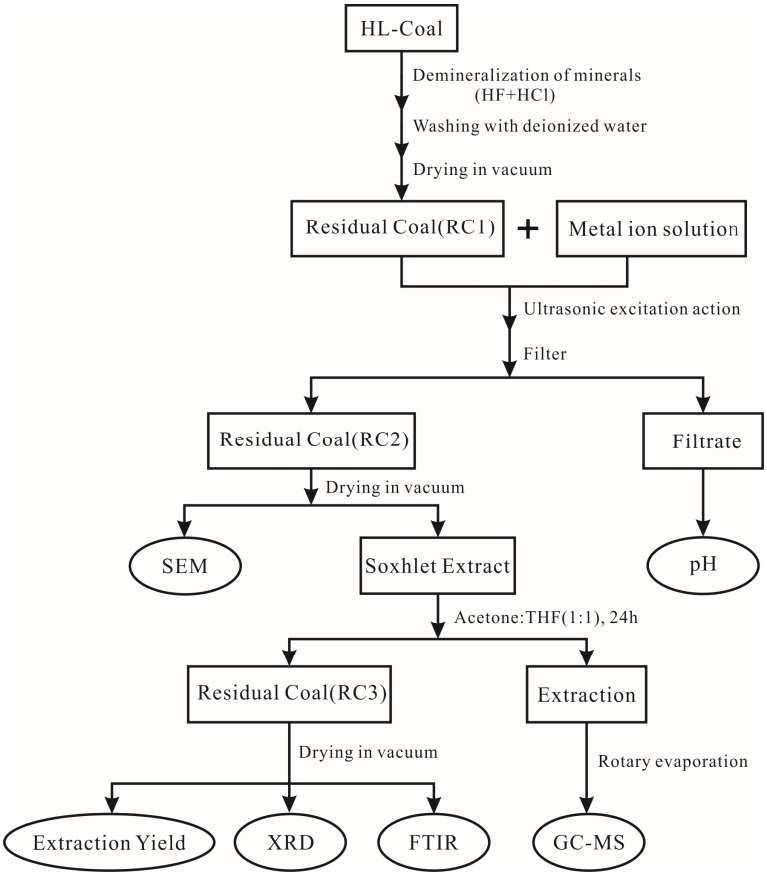

Figure 1. Experimental flow chart.

2.4. Organic Matter Extraction Experiment

The prepared coal samples loaded with different metal ions under ultrasonic treatment, including the coal samples from the control group, were placed in filter paper sleeves. The upper end was sealed with a plug of defatted cotton and then placed into a Soxhlet extraction apparatus containing the extraction solvent. Each coal sample weighed 5 g, and the extraction solvent volume was 250 milliliters. The selected extraction solvents were acetone and tetrahydrofuran (THF) in a 1:1 volume ratio. Acetone was chosen for its effectiveness in extracting lightweight components from coal, while THF was selected for its effectiveness in extracting heavier components. The extraction process was carried out for 24 h at a temperature of 76 °C. Prior to the experiment, all the solvents used were distilled and purified, and the equipment was rinsed with the solvents 2–3 times to ensure cleanliness and purity.

After 24 h of Soxhlet extraction, the extraction solvent containing the extracted compounds was concentrated to a volume of 3–4 mL using a rotary evaporator. Subsequently, it was further concentrated to 1 mL under a stream of nitrogen gas. This concentrated extract was then used for the GC-MS analysis. The calculation of organic matter extraction efficiency was performed using a weighing method. Specifically, the coal samples before and after extraction were dried at 80 °C for 12 h, and their weights were recorded. The organic compound extraction efficiency was calculated using Equation (1), which compares the mass change of the coal sample before and after extraction:

$$\text{Extraction Yield}(\%) = \frac{\text{RC2(g)} - \text{RC3(g)}}{\text{RC2(g)}} \times 100 \quad (1)$$

2.5. GC/MS Test Analysis

Organic compound detection was performed at Shaanxi Provincial Key Laboratory of Geological Support for Coal Green Exploitation using an Agilent GC-MS instrument with the model number 7890B-5977B. The chromatographic column used was a DB-1MS column (60 m × 0.25 mm × 0.25 μm). The experimental conditions and methods followed were those of the literature [17]. The data were acquired in full-scan mode and processed using MassHunter Workstation version 10.0.368. Identification of the compound types was accomplished by comparing the peak retention times with the standard compounds and by using mass spectrometric analysis and the reference literature [17,35].

The relative content of different substances in the extracted organic matter was calculated using the peak area normalization method. The proportions of different components representing the substance's content were calculated using Equation (2):

$$P = \frac{\sum_{i=1}^{n} Si}{S} \quad (2)$$

In the equation provided, P represents the proportions of a specific component, S represents the total peak area of the compounds, Si represents the peak area of a specific type of compound, and n represents the number of compounds within each component.

2.6. Fourier Transform Infrared Spectroscopy

The remaining coal samples, obtained after the extraction of different metal ion-loaded coal samples using ultrasound, were subjected to WQF-530 Fourier transform infrared spectroscopy (FTIR) analysis. The procedure was as follows:

1. Approximately 100 mg of potassium bromide, dried in a vacuum oven at 100 °C for 10 h, was weighed and placed into an agate mortar. A small amount of coal sample, which had undergone drying treatment, was thoroughly mixed with the potassium bromide. The mixture was then ground finely.
2. The mixture was placed into a mold and subjected to vacuum pressure on a tablet press at 20–25 MPa for 1 min.
3. The mold containing a transparent circular thin sheet with a thickness of 0.1–1.0 mm was fixed onto a sample holder.
4. Infrared spectroscopy was conducted on the samples using the FTIR spectrometer. The experimental parameters were set as follows: a wavenumber range from 4400 to 400 cm^{-1} and a resolution of 2 cm^{-1}.

2.7. X-ray Diffraction

The remaining coal samples, obtained after the extraction of different metal ion-loaded coal samples using ultrasound, were subjected to X-ray diffraction (XRD) testing using a German Bruker D8 X-ray diffractometer. The sample preparation method used an aluminum frame. The experimental parameters were set as follows: copper (Cu) target radiation was used. The voltage was set at 40 kV, and the current at 40 mA. The scanning range was from 10 to 80°. The scanning speed was 5°/min. The X-ray wavelength was 0.154178 nm. The divergence and anti-scattering slits were set at 1.0 mm, and the receiving slit was set at 0.2 mm.

3. Results and Discussion

3.1. Extraction Analysis

Through the weighing method, it can be determined that there are variations in the efficiency of the extraction of organic matter from coal samples loaded with different metal ions under ultrasonic treatment (Figure 2). As shown in Figure 2, in the absence of metal ions (blank control group), the extraction rate of small organic molecules from the tar-rich coal is 2.5%. However, when the coal samples are loaded with the metal ions Mn^{2+}, Co^{2+}, Cu^{2+}, Fe^{2+}, and Ni^{2+} under ultrasonic conditions, the extraction rates of the small organic

molecules are 7.8%, 3.4%, 2.6%, 3.1%, and 4.6%, respectively. The comparison reveals that the ultrasonic loading of different metal ions has an impact on the extraction rate of small organic molecules from tar-rich coal. Compared to the blank control group, the ultrasonic loading of various metal ions results in a noticeable increase in the extraction rate of small organic molecules from tar-rich coal. Among them, the extraction rate from the coal sample exhibits the most significant increase under the ultrasonic loading of Mn^{2+}, with an increment of up to 212%. Ni^{2+} follows with a lesser increase, and Cu^{2+} exhibits the smallest enhancement with only a 2% increase.

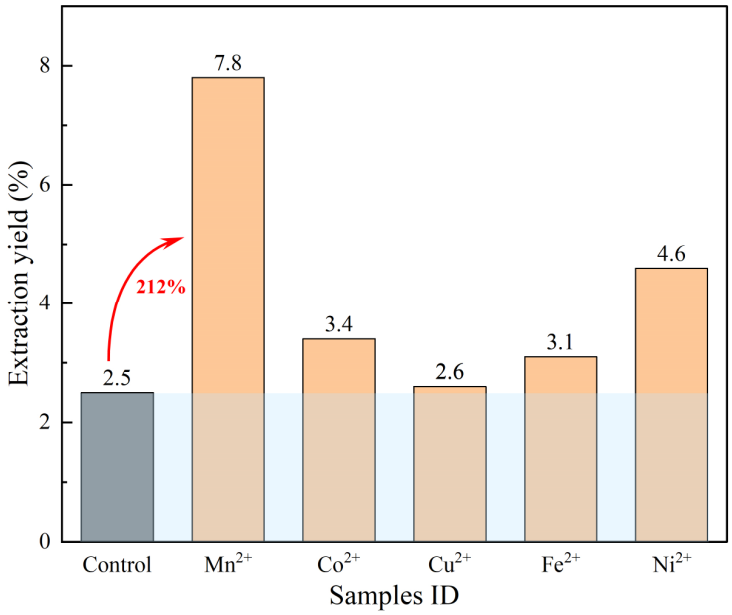

Figure 2. Extraction rates of small organic molecules from tar-rich coal loaded with various metal ions under ultrasound treatment.

The organic composition differences in small organic molecules extracted after ultrasonic loading with various metal ions were analyzed using GC-MS. The mass spectra of the small organic molecules extracted after ultrasonic loading with different metal ions are shown in Figure 3. The quantification of the content proportion of different compound classes in the extracted small organic molecules from tar-rich coal loaded with various metal ions is presented in Figure 4, following Equation (2). From the results shown in Figure 3, it is evident that the carbon number range of small organic molecules extracted after ultrasonic loading with different metal ions spans from C_7 to C_{33}. In comparison, in the absence of metal ions (blank control group), the extracted small organic molecules have a carbon number range from C_7 to C_{24}. Other metal ions also lead to an expansion in the carbon number range of the extracted small organic molecules, with differences primarily in the extent of the expansion. In Figure 3, the NIST compound library was used for nomenclature analysis, and recognizable peaks of the normal alkanes in the mass spectra of the small organic molecules extracted after ultrasonic loading with different metal ions were annotated. The envelope curves indicate overall differences in peak shapes. Comparatively, in the absence of metal ions (blank control group), after ultrasonic loading with different metal ions, the envelope curves of the normal alkane peaks in the extracted small organic molecules exhibit phenomena such as peak shifting (left shift of peak-I within Mn^{2+} and peak-II within Ni^{2+}), and new peaks appear within Mn^{2+}, Cu^{2+}, Fe^{2+}, and Ni^{2+}.

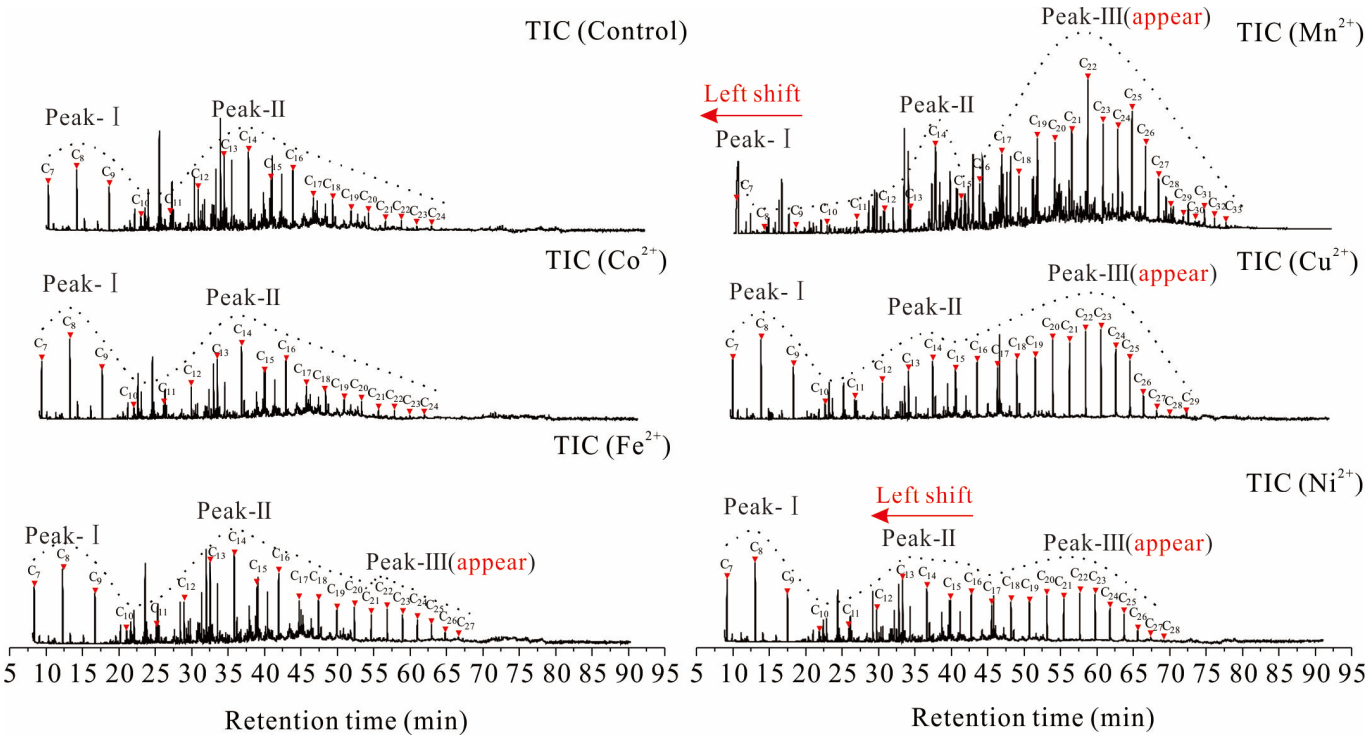

Figure 3. Total ion current (TIC) mass spectra of extracted small organic molecules from tar-rich coal loaded with various metal ions under ultrasound treatment.

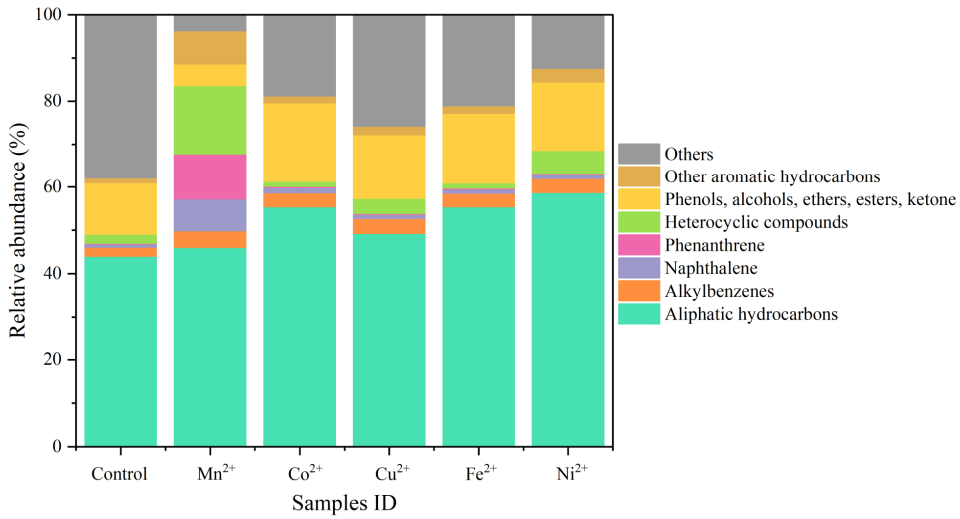

Figure 4. Composition of content proportions of typical compound classes in extracted small organic molecules from tar-rich coal loaded with different metal ions under ultrasound treatment.

Figure 4 reveals that in the absence of metal ions (blank control group), the predominant compound class in the extracted small organic molecule phase from the tar-rich coal is aliphatic hydrocarbons, accounting for 43.99% of the total. Following the aliphatic hydrocarbons, the combined percentages of phenols, alcohols, ethers, esters, and ketones amount to 11.86%. The content proportions of the alkylbenzenes, naphthalene, phenanthrene, heterocyclic compounds, and other aromatic hydrocarbons are 2.04%, 0.74%, 0.17%, 2.14%, and 1.10%, respectively. In comparison, when different metal ions are present and subjected to ultrasonic loading, there are slight variations in the content proportions of the different compound classes in the corresponding extracted small organic molecule phases.

This suggests that the ultrasonic loading process with different metal ions may result in differences in the binding sites and strengths of the interaction with coal.

Overall, it can be observed that after ultrasonic loading with different metal ions, the content proportions of the aliphatic hydrocarbons, alkylbenzenes, naphthalene, phenanthrene, and other aromatic hydrocarbons in the extracted small organic molecule phase from the coal samples increase. Among these, the ultrasonic loading of Mn^{2+} induces the most significant changes in the content proportions of the various compound classes. In comparison to the blank control group, the content proportions of the aliphatic hydrocarbons and alkylbenzenes in the extracted small organic molecule phase increase to a lesser extent, with values of 45.99% and 3.84%, respectively. Conversely, the proportions of phenols, alcohols, ethers, esters, and ketones decrease to 5.02%. Notably, the content proportions of naphthalene, phenanthrene, heterocyclic compounds, and other aromatic hydrocarbons increase significantly, reaching proportions of 7.36%, 10.55%, 15.83%, and 7.71%, respectively. Overall, the content proportions of the different compound classes become more balanced.

However, when the metal ions are Co^{2+}, Cu^{2+}, Fe^{2+}, or Ni^{2+}, the content proportions of the aliphatic hydrocarbons range from 49.23% to 58.67%, the alkylbenzenes range from 3.12% to 3.28%, the naphthalene range from 0.86% to 1.17%, the phenanthrene range from 0.24% to 0.29%, the heterocyclic compounds range from 2.19% to 5.29%, and the proportions of the phenols, alcohols, ethers, esters, ketone, and the like range from 14.90% to 18.31%. The content proportions of the other aromatic hydrocarbons range from 1.61% to 3.19%. After ultrasonic loading with metal ions, there is an increase in the content proportions of the aliphatic hydrocarbons, heterocyclic compounds, naphthalene, phenanthrene, and other aromatic hydrocarbons. In summary, the loading of metal ions has a promoting effect on the extraction of aromatic compounds and heterocyclic compounds. This results in a more comprehensive composition of organic small molecules that can be extracted from tar-rich coal, with more balanced content proportions for each compound class.

3.2. Structural Analysis of Raffinate Coal

3.2.1. Fourier Transform Infrared Spectroscopy Analysis

In this study, the infrared spectra of all the extracted residual coals were divided into four main regions to compare and analyze the functional group characteristics:

1. 3600–3000 cm^{-1}: Characteristic absorption peaks of hydroxyl groups.
2. 3000–2800 cm^{-1}: Characteristic absorption peaks of aliphatic hydrocarbons.
3. 1800–1000 cm^{-1}: Characteristic absorption peaks of oxygen-containing functional groups.
4. 900–700 cm^{-1}: Characteristic absorption peaks of aromatic hydrocarbons (see Figure 5) [38,39].

As shown in Figure 5, compared to the blank control group, the changes in response intensity in the spectral profiles of residual coals loaded with different metal ions primarily manifest in the aliphatic C-H_n, oxygen-containing functional groups and the hydroxyl groups. The changes in aliphatic C-H_n are particularly noticeable, with significantly reduced peak areas. This indicates that after ultrasonic loading with different metal ions, the organic compounds in tar-rich coal undergo a transformation process. It is speculated that there are intermediate processes, such as the chain breaking of aliphatic substances, accompanied by the detachment of small-molecule aromatics from coal, the decomposition and transformation of carboxyl groups and ether bonds, ion exchange, and potential changes in hydrogen bonding through the self-association of the hydroxyl groups.

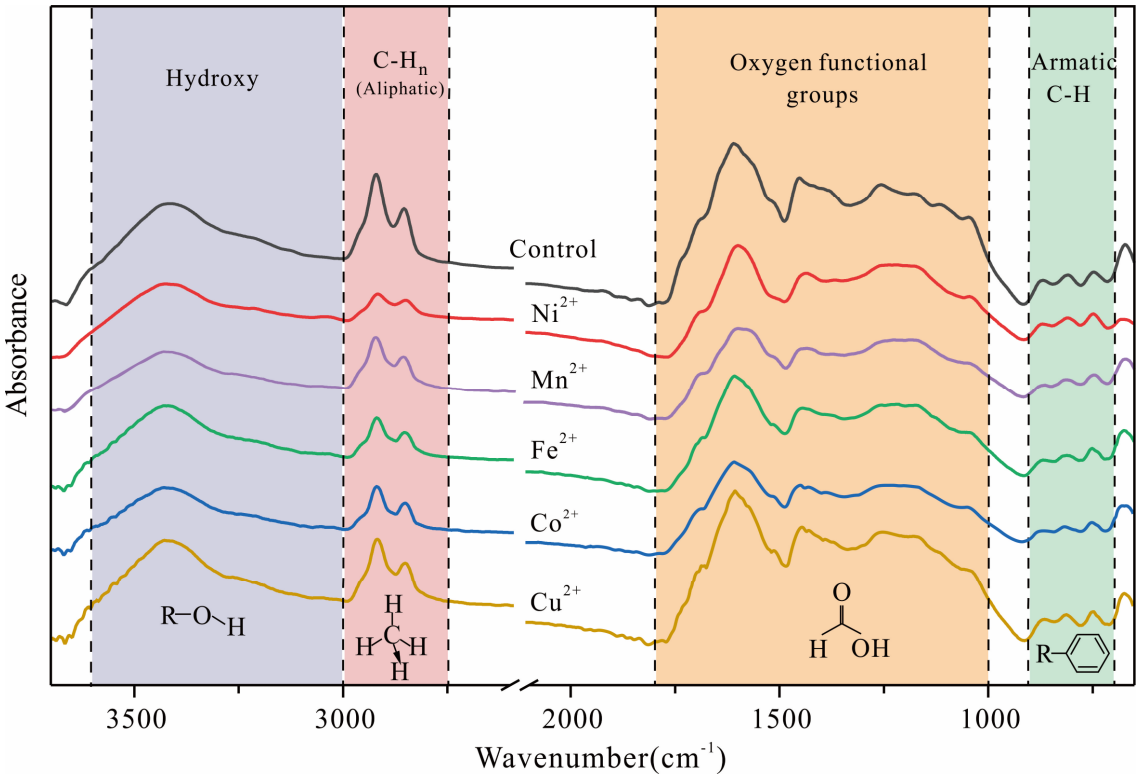

Figure 5. Infrared spectra of extracted residual coals.

To further elucidate the characteristics of the functional group changes in the residual coals loaded with different metal ions, according to references [40–44], we employed Origin 2021 software to perform peak fitting on the obtained FTIR spectra of the different coal samples separately in the four major spectral regions. This was conducted to achieve a semi-quantitative analysis of the functional group changes in the residual coal. The peak fitting results for the blank control group are shown in Figure 6, while the peak fitting for the residual coals extracted from the coal samples loaded with different metal ions was also carried out following the same procedure as that shown in Figure 6. The detailed fitting process is not presented here, and the final calculated structural parameters are summarized in Table 2. Comparing the calculated structural parameter results for different residual coals (Table 2), it becomes evident that after ultrasonic loading with metal ions, the coal samples experience an increase in the length of aliphatic chains (F) and a reduction in branching; a decrease in hydrogen richness (I_H); a decrease in aromatic hydrogen content ($F_{AR}{}^H$); an increase in the degree of condensation (DOC); and an increase in aromaticity (AR). The increase in the length of the aliphatic chains (F) extracted from the residual coal indicates that after the ultrasonic loading of metal ions, the fat in coal is easily extracted due to a loose structure and chain-breaking reaction processes. This finding is consistent with the increased proportion of aliphatic hydrocarbons in the extract. Additionally, the decrease in hydrogen richness (I_H) and the content of aromatic hydrogen ($F_{AR}{}^H$) in residual coal also corresponds to an increase in the proportion of naphthalene and phenanthrene aromatics in the extract. The changes observed in the molecular structure parameters within the extracted residual coal align with the variations seen in the proportion of small molecular components extracted, providing strong evidence for the impact of ultrasonically loaded metal ions on the extraction of small molecular phases from tar-rich coal.

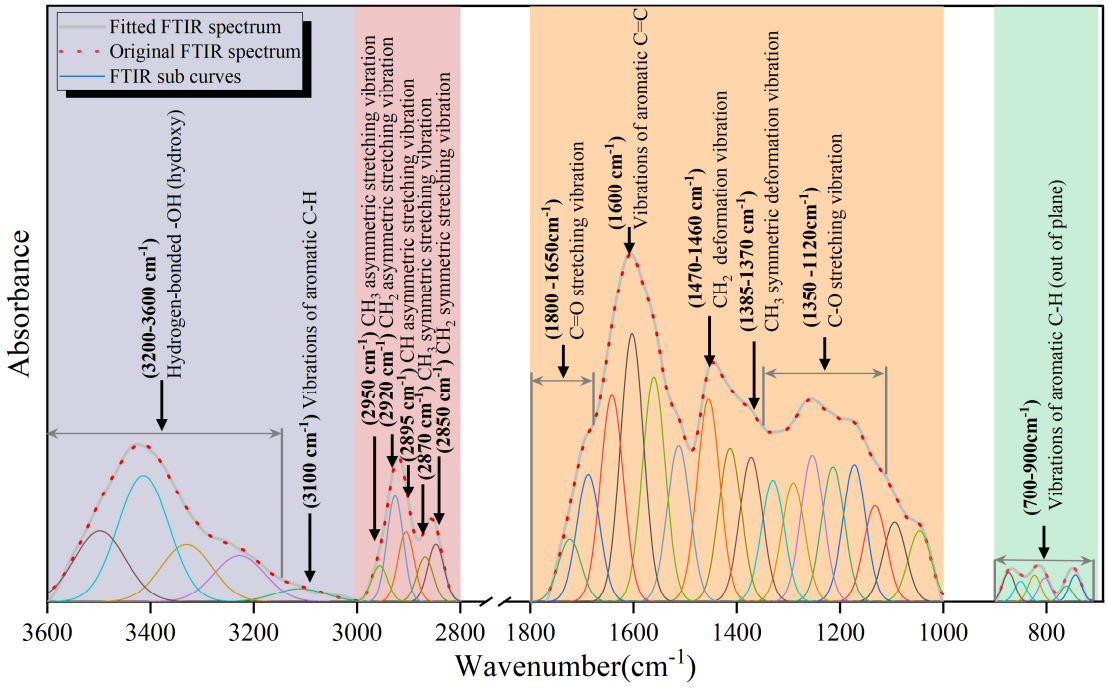

Figure 6. Peak fitting of infrared spectra of extracted residual coals (exemplified with blank control group).

Table 2. Semi-quantitative parameters of infrared spectra for extracted residual coals.

Sample ID	F	I_H	$F_{AR}{}^H$	DOC	AR
Control	2.8007	0.1915	0.4273	0.1307	0.2164
Co^{2+}	2.8528	0.0886	0.2583	0.2044	0.7462
Mn^{2+}	3.7552	0.1057	0.1779	0.1578	0.5192
Fe^{2+}	3.3470	0.1299	0.3418	0.1578	0.4276
Ni^{2+}	3.6536	0.1486	0.2308	0.1406	0.3001
Cu^{2+}	2.9102	0.1534	0.2995	0.1590	0.3483

Note: Length of aliphatic chains (F): $F = \frac{CH_2}{CH_3} = \frac{A(2935\text{-}2915\ cm^{-1})}{A(2975\text{-}2950\ cm^{-1})}$; hydrogen richness ($I_H$): $I_H = \frac{A(2915\text{-}2935\ cm^{-1})}{A(1620\text{-}1550\ cm^{-1})}$; aromatic hydrogen content ($F_{AR}{}^H$): $F_{AR}^H = \frac{H_{ar}}{H} = \frac{A(900\text{-}700\ cm^{-1})}{A(900\text{-}700\ c\,m^{-1})+A(3000\text{-}2800\ cm^{-1})}$; degree of condensation (DOC): $DOC = \frac{A(900\text{-}700\ cm^{-1})}{A(1620\text{-}1550\ cm^{-1})}$; aromaticity (AR): $AR = \frac{A(900\text{-}700\ cm^{-1})}{A(3000\text{-}2800\ cm^{-1})}$.

3.2.2. X-ray Diffraction Analysis

The XRD test results for all extracted residual coals are presented in Figure 7. Based on this, using Origin 8.5 software, we conducted peak fitting for three characteristic peaks: the γ band, the 002 peak (20°–30°), and the 100 peak (40°–50°) [44,45]. Subsequently, we calculated the interlayer spacing (d_{002}), expansivity (L_a), stacking height (L_c), and the number of stacked layers (N_{ave}) using the respective formulas. The calculated structural parameters are summarized in Table 3.

From Table 3, it can be observed that, in comparison with the blank control group, after ultrasonic loading with different metal ions, several changes occur in the extracted residual coals. The interlayer spacing (d_{002}) between aromatic layers decreases, stacking height (L_c) increases, expansivity (L_a) increases, and the number of stacked layers (N_{ave}) decreases. After ultrasonic loading with metal ions, the extraction rate of small-molecule components from tar-rich coal significantly increases. Moreover, the proportions of aliphatic hydrocarbons, heterocyclic compounds, naphthalene, phenanthrene, and other aromatic hydrocarbons in the extracted materials increase. This indicates that the loading of metal ions enhances the extraction of small-molecule compounds and increases the likelihood of coal macromolecular restructuring. Consequently, the vertical distance between aromatic

layers in the residual coal decreases, leading to an increase in vertical stacking height and, thus, an increase in the number of stacked layers between aromatic layers. The decrease in the branching of the aliphatic chains and the reduction in the oxygen-containing functional groups in the residual coal result in an effective increase in the planar expansibility of the aromatic structural system, leading to an increase in expansivity (L_a).

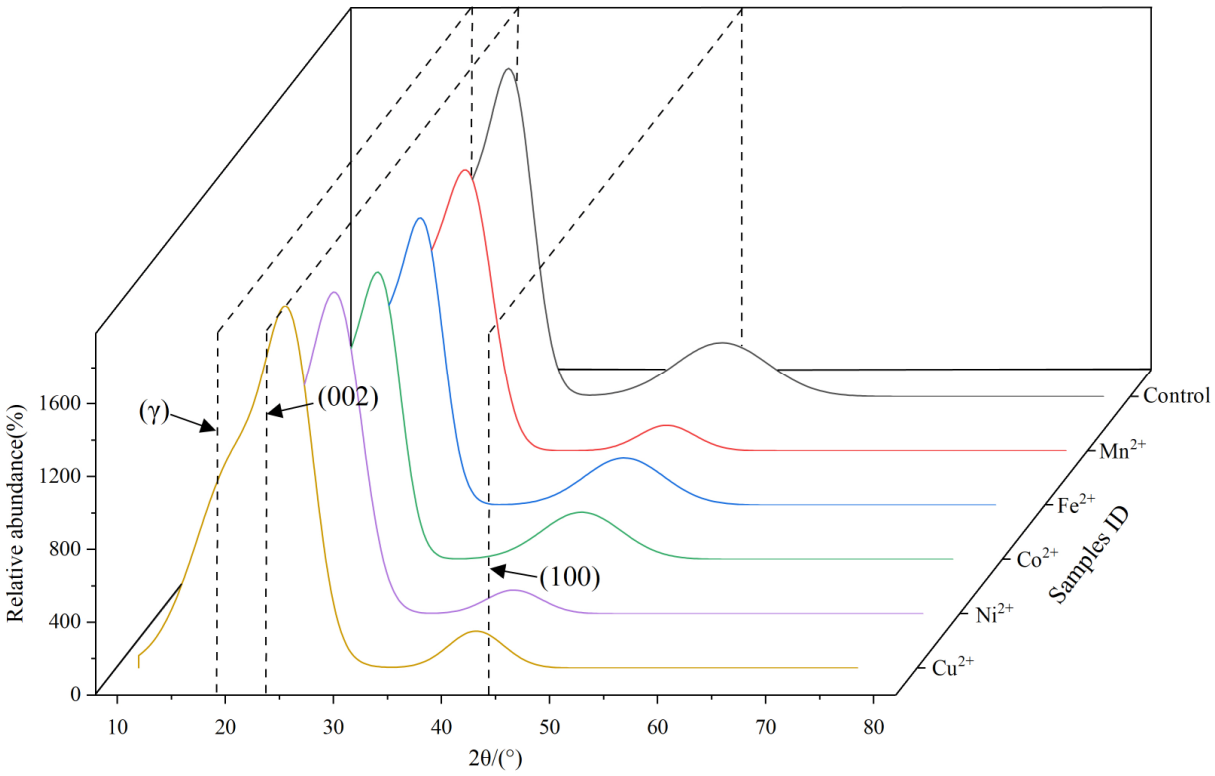

Figure 7. XRD spectra of extracted residual coals.

Table 3. XRD structural parameters of coal samples.

Sample ID	d_{002}/nm	L_a/nm	L_c/nm	N_{ave} (Layers)
Control	0.3593	1.7235	1.4893	4.1450
Co^{2+}	0.3538	1.8137	1.6498	4.6631
Fe^{2+}	0.3560	2.1343	1.6348	4.5921
Ni^{2+}	0.3532	2.8315	1.8459	5.2262
Cu^{2+}	0.3573	2.7578	1.5709	4.3966
Mn^{2+}	0.3532	2.8648	1.8990	5.3766

Note: $d_{002} = \lambda/(2\mathrm{Sin}\theta_{002})$; $L_c = 0.9\lambda/(\beta_{002}\cos\theta_{002})$; $L_a = 1.84\lambda/(\beta_{100}\cos\theta_{100})$; $N_{ave} = L_c/d_{002}$; λ represents the wavelength of incident light at 0.154056 nm; β_{002} and β_{100} are the fitted half-widths of the 002 and 100 diffraction peaks, respectively; θ_{002} is the diffraction angle corresponding to the maximum diffraction peak of the 002-crystal plane index, and θ_{100} is the diffraction angle corresponding to the maximum diffraction peak of the 100-crystal plane index.

3.3. Mechanism Analysis

After ultrasonic loading with metal ions, the increased proportion of naphthalene, phenanthrene, and other aromatic hydrocarbons suggests that the presence of metal ions has a certain catalytic promotion effect on the extraction of aromatic compounds. This leads to a greater diversity of organic compounds that can be extracted from tar-rich coal (Figure 4). The length of the aliphatic chains in the residual coal matrix increased, while the degree of branching (F) decreased. The degree of hydrogen enrichment (I_H) decreased, and the aromatic hydrogen ratio ($F_{AR}{}^H$) also decreased, as confirmed by the results (Table 2). Simultaneously, after ultrasonic loading with different metal ions, the

interlayer spacing d_{002} in the extracted residual coal decreased, while the expansivity L_a increased; the stacking degree L_c increased, and the number of stacking layers N_{ave} decreased (Table 3). These observations provide indirect insights into the changes and mechanisms involved in the extraction of small organic phases following the loading of metal ions.

After subjecting the tar-rich coal to ultrasonic loading with various metal ions, a comparison with the control group reveals that the surface of tar-rich coal becomes rougher and exhibits an overall increase in porosity. This enhanced porosity facilitates optimal contact and interaction between solvents during the extraction process of small organic components (Figure 8). Additionally, the ion exchange interactions occurring between the metal ions and the coal matrix result in the chemical adsorption of some metal ions onto the hydroxyl and carboxyl groups within the coal molecules. Consequently, this significantly increases the concentration of H^+ in the aqueous solution. When combined with the abundant Cl^- accompanying the addition of metal ions, it ultimately leads to a substantial decrease in the pH of the leaching aqueous solution (Figure 9). Simultaneously, metal ions concurrently act as a catalyst due to their positive charge, which strongly attracts negative charges in coal. Consequently, this diminishes the charge transfer ability within coal and weakens the π-π bond between condensed aromatics. As a result, internal small molecules become more susceptible to dissolution in the solvent, thereby facilitating the extraction of naphthalene, phenanthrene, and other small aromatic hydrocarbons. Consequently, the combined effect of ion exchange and catalysis can enhance the extraction efficiency of the low- to medium-molecular-weight fraction in tar-rich coal (Figure 10). Among these observations, the impact of Mn^{2+} loading on the extraction of small organic phases in tar-rich coal is the most significant. This may be attributed to the smaller radius of Mn^{2+} compared to the other four ions, making it easier for Mn^{2+} to form coordination compounds with electron-donating ligands in the coal, thereby enhancing the ion catalysis effects. This coordination results in the disruption of hydrogen bonds and π-π bonds, as substantiated by the infrared spectroscopy test results (Figure 5).

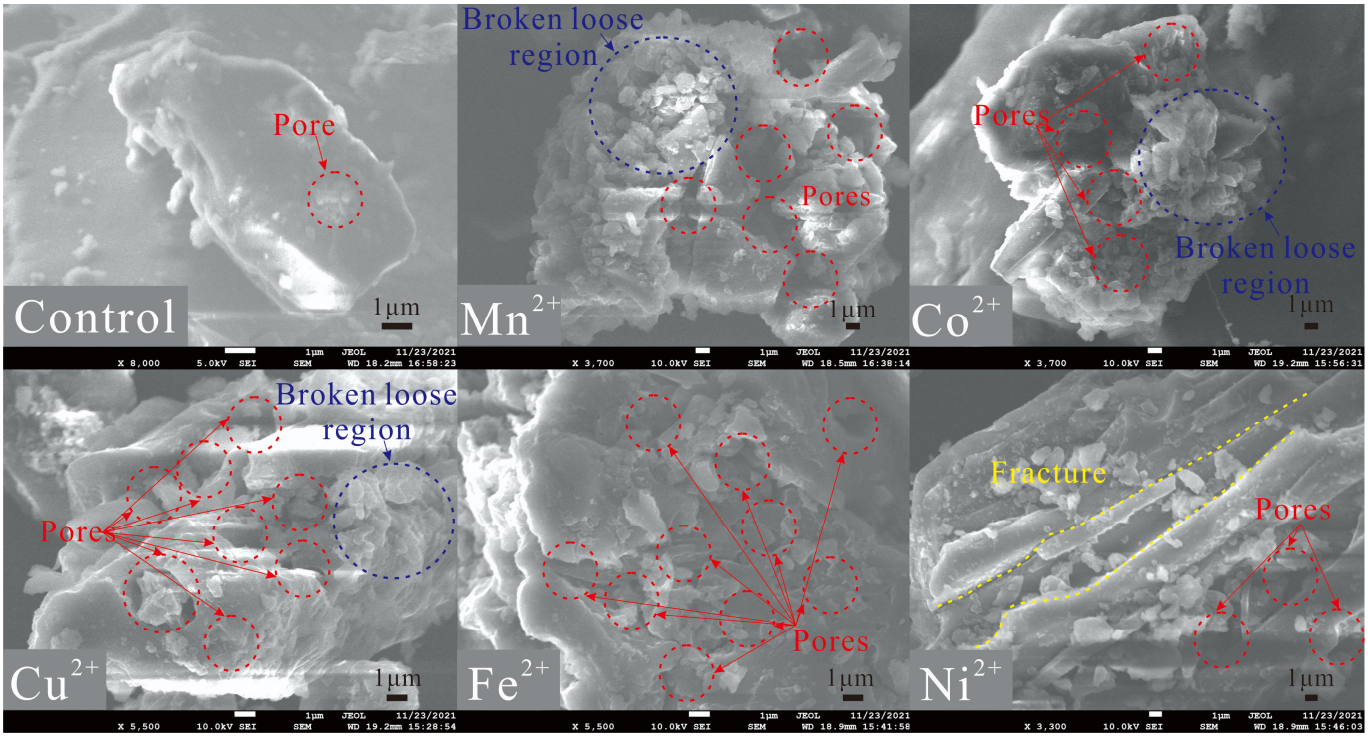

Figure 8. Scanning electron microscopy (SEM) of tar-rich coal after ultrasonic loading with different metal ions.

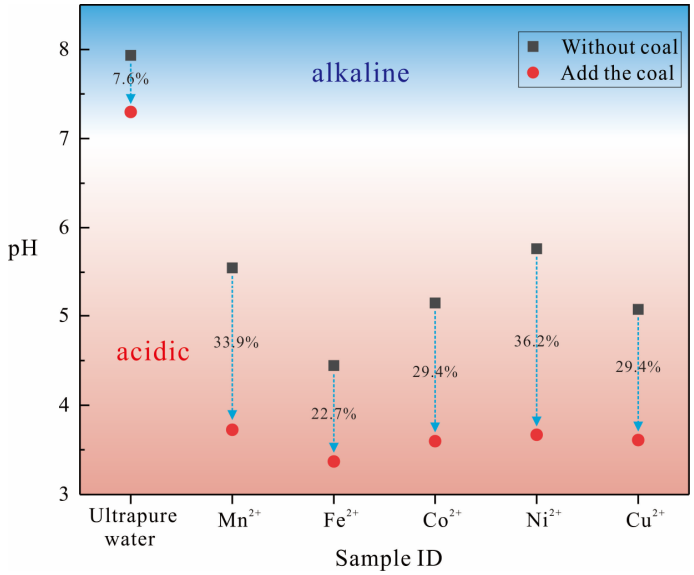

Figure 9. The leaching solution's pH change of tar-rich coal after ultrasonic loading with different metal ions.

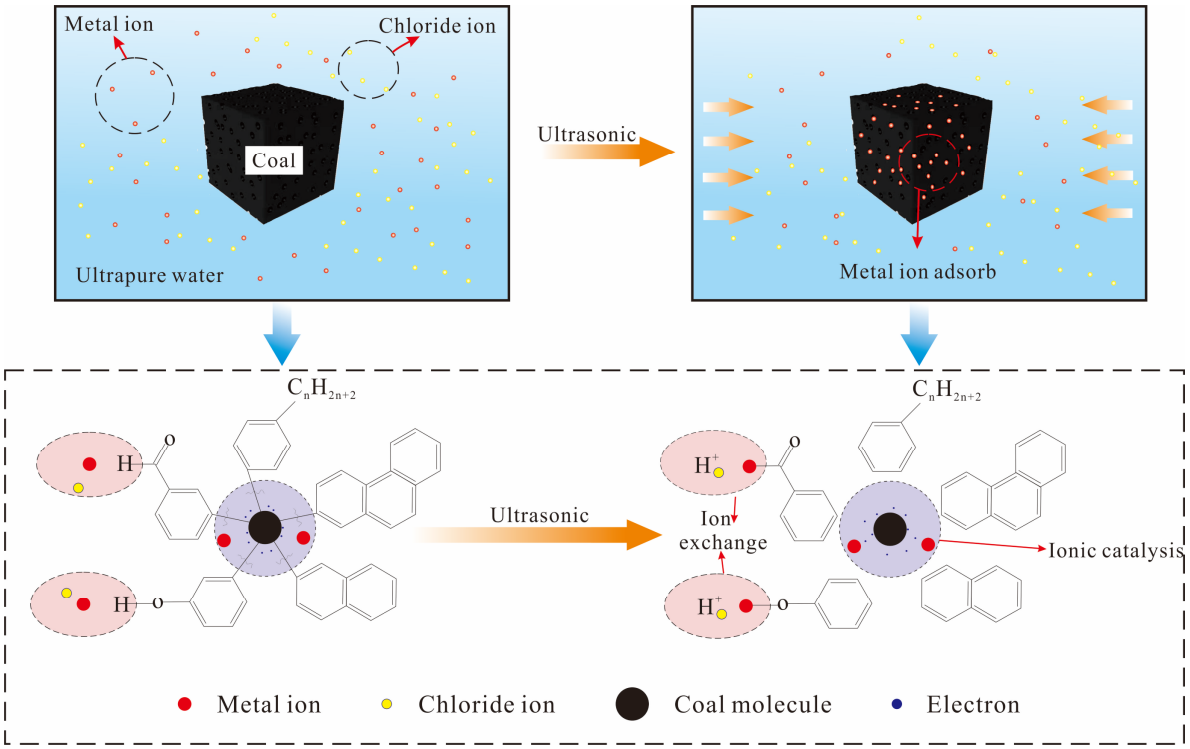

Figure 10. Reaction mechanism of tar-rich coal after ultrasonic loading with different metal ions.

4. Conclusions

Conclusions were drawn from the analysis of extractable low-molecular-weight fractions and residual coal products in tar-rich coal samples from the Huangling mining area of the Ordos Basin after ultrasonic treatment with various metal ions.

1. Under ultrasonic treatment, Mn^{2+}, Co^{2+}, Cu^{2+}, Fe^{2+}, and Ni^{2+} metal ions enhanced the extraction efficiency of organic low-molecular-weight fractions. Among these metal ions, Mn^{2+} exhibited the most significant effect, resulting in a remarkable 212% increase in the extraction rate compared to the blank control group. Following the ultrasonic treatment with different metal ions, there were observable shifts in the

peak positions and a number range for normal alkanes present within low-molecular-weight fractions. Additionally, the proportions of aliphatic hydrocarbons, alkylbenzenes, naphthalene, phenanthrene, and other aromatic hydrocarbons increased within this extracted organic fraction obtained from coal samples.

2. After subjecting the residual coal samples to ultrasonic loading with various metal ions, consistent trends in the chemical changes were observed. Specifically, there was an increase in the length of aliphatic chains, a decrease in branching (F), a decrease in hydrogen richness (I_H), a decrease in aromatic hydrogen content ($F_{AR}{}^H$), an increase in the degree of condensation (DOC), and an increase in aromaticity (AR). Furthermore, the interlayer spacing (d_{002}) within the aromatic structure decreased, while the stacking degree (L_c) increased, and both the expansivity (L_a) and the number of stacked layers (N_{ave}) decreased.
3. After subjecting the coal to ultrasonic loading with various metal ions, the surface of tar-rich coal becomes rougher and exhibits an overall increase in porosity. The metal ions undergo ion exchange with the hydrogen ions present in the coal, thereby altering and influencing the chemical structure of certain functional groups within the coal. Moreover, these metal ions adsorbed onto the coal molecules and effectively formed complexes with unbound electrons within the small molecules of the coal; thus, catalytic effects were facilitated.

Author Contributions: Y.B. conceived and designed the experiments, initiated the project, and performed the experiments; Z.W. analyzed the data, collected the literature, and created the figures; Y.B., C.W. and Y.H. revised the manuscript; Z.W. wrote the paper. All authors have read and agreed to the published version of the manuscript.

Funding: This research was funded by the National Natural Science Foundation of China (Nos. 42172200 & 41972183).

Data Availability Statement: Data will be made available on request.

Conflicts of Interest: The authors declare no conflicts of interest.

References

1. Shi, Q.; Li, C.; Wang, S.; Li, D.; Wang, S.; Du, F.; Qiao, J.; Cheng, Q. Effect of the depositional environment on the formation of tar-rich coal: A case study in the northeastern Ordos Basin, China. *J. Petrol. Sci. Eng.* **2022**, *216*, 110828. [CrossRef]
2. Ju, Y.; Zhu, Y.; Zhou, H.; Ge, S.; Xie, H. Microwave pyrolysis and its applications to the in situ recovery and conversion of oil from tar-rich coal: An overview on fundamentals, methods, and challenges. *Energy Rep.* **2021**, *7*, 523–536. [CrossRef]
3. Du, Z.; Li, W. The catalytic effect from alkaline elements on the tar-rich coal pyrolysis. *Catalysts* **2022**, *12*, 376. [CrossRef]
4. Ju, Y.; Zhu, Y.; Zhang, Y.; Zhou, H.; Peng, S.; Ge, S. Effects of high-power microwave irradiation on tar-rich coal for realising in situ pyrolysis, fragmentation, and low-carbon utilisation of tar-rich coal. *Int. J. Rock Mech. Min.* **2022**, *157*, 105165. [CrossRef]
5. Abdelsayed, V.; Shekhawat, D.; Smith, M.W.; Link, D.; Stiegman, A.E. Microwave-assisted pyrolysis of Mississippi coal: A comparative study with conventional pyrolysis. *Fuel* **2018**, *217*, 656–667. [CrossRef]
6. Pan, J.; Lv, M.; Bai, H.; Hou, Q.; Li, M. Effects of metamorphism and deformation on the coal macromolecular structure by laser Raman spectroscopy. *Energ. Fuel* **2017**, *31*, 1136–1146. [CrossRef]
7. Iino, M. Network structure of coals and association behavior of coal-derived materials. *Fuel Process. Technol.* **2000**, *62*, 89–101. [CrossRef]
8. Suzuki, M.; Norinaga, K.; Iino, M. Macroscopic observation of thermal behavior of concentrated solution of coal extracts. *Fuel* **2004**, *83*, 2177–2182. [CrossRef]
9. He, W.; Liu, Z.; Liu, Q.; Shi, L.; Shi, X. Behavior of radicals during solvent extraction of three low rank bituminous coals. *Fuel Process. Technol.* **2017**, *156*, 221–227. [CrossRef]
10. Li, Z.K.; Wei, X.Y.; Yang, Z.S.; Yan, H.L.; Wei, Z.H. Characterization of extracts from geting bituminous coal. *Anal. Lett.* **2015**, *48*, 1494–1501. [CrossRef]
11. Kim, K.; Cho, H.; Lee, S.; Mun, M.; Lee, D. Coal and solvent properties and their correlation with extraction yield under mild conditions. *Korean J. Chem. Eng.* **2016**, *33*, 2142–2159. [CrossRef]
12. Li, F.J.; Wei, X.Y.; Fan, M.H.; Zong, Z.M. Separation and structural characterization of the value-added chemicals from mild degradation of lignites: A review. *Appl. Energ.* **2016**, *170*, 415–436. [CrossRef]
13. Lu, H.Y.; Wei, X.Y.; Yu, R.; Peng, Y.L. Sequential thermal dissolution of Huolinguole lignite in methanol and ethanol. *Energ. Fuel* **2011**, *25*, 2741–2745. [CrossRef]

14. Marzec, A. Towards an understanding of the coal structure: A review. *Fuel Process. Technol.* **2002**, *77–78*, 25–32. [CrossRef]
15. Marta, K. Coal structure studied by means of molecular acoustics methods. *Fuel Process. Technol.* **2002**, *77–78*, 33–43. [CrossRef]
16. Liu, X.; Song, D.; He, X.; Nie, B.; Wang, L. Insight into the macromolecular structural differences between hard coal and deformed soft coal. *Fuel* **2019**, *245*, 188–197. [CrossRef]
17. Bao, Y.; Hu, Y.; Huang, H.; Meng, J.; Zheng, R. Evidence of coal biodegradation from coalbed-produced water—A case study of Dafosi gas field, Ordos Basin, China. *ACS Omega* **2023**, *8*, 41885–41896. [CrossRef]
18. Pajak, J.; Marzec, A.; Severin, D. Compositions of solvent-extracts of a Polish bituminous coal. *Fuel* **1985**, *64*, 64–67. [CrossRef]
19. Ji, H.; Li, Z.; Peng, Y.; Yang, Y.; Tang, Y.; Liu, Z. Pore structures and methane sorption characteristics of coal after extraction with tetrahydrofuran. *J. Natural Gas Sci. Eng.* **2014**, *19*, 287–294. [CrossRef]
20. Vorob'yeva, N.S.; Zemskova, Z.K.; Bodzek, D.; Kiselev, V.I.; Petrov, A.I.A. Hydrocarbons of the soluble part of coal. *Petrol. Chem. U.S.S.R.* **1983**, *23*, 232–239. [CrossRef]
21. Bodzek, D.; Marzec, A. Molecular components of coal and coal structure. *Fuel* **1981**, *60*, 47–51. [CrossRef]
22. Wargadalam, V.J.; Norinaga, K.; Iino, M. Hydrodynamic properties of coal extracts in pyridine. *Energ. Fuel* **2001**, *15*, 1123–1128. [CrossRef]
23. Klotzkin, M.P. Solvent treatment of coals: 1. Effects on microporosity at ambient temperature. *Fuel* **1985**, *64*, 1092–1096. [CrossRef]
24. Klotzkin, M.P. Solvent treatment of coals. 2. Effects on microporosity of extractions in the presence of ultrasonic energy. *Fuel* **1985**, *67*, 104–108. [CrossRef]
25. Liu, Y.; Yan, L.; Lv, P.; Ren, L.; Kong, J.; Wang, J.; Li, F.; Bai, Y. Effect of n-hexane extraction on the formation of light aromatics from coal pyrolysis and catalytic upgrading. *J. Energy Inst.* **2020**, *93*, 1242–1249. [CrossRef]
26. Hu, R.N.; Wang, Z.C.; Li, L.; Wang, X.; Pan, C.; Kang, S.; Ren, S.; Lei, Z.; Shui, H. Effect of solvent extraction pretreatments on the variation of macromolecular structure of low rank coals. *J. Fuel Chem. Technol.* **2018**, *46*, 778–786. [CrossRef]
27. Yang, Z.; Li, Y.; Xue, W.; Yin, Z.; Meng, Z.; Zhou, A. Small molecules from multistep extraction of coal and their effects on coal adsorption of CH_4. *Catal. Today* **2021**, *374*, 192–199. [CrossRef]
28. Ma, Y.; Ma, F.; Mo, W.; Wang, Q. Five-stage sequential extraction of Hefeng coal and direct liquefaction performance of the extraction residue. *Fuel* **2020**, *266*, 117039. [CrossRef]
29. Sönmez, Ö.; Yıldız, Ö.; Çakır, M.Ö.; Gözmen, B.; Giray, E.S. Influence of the addition of various ionic liquids on coal extraction with NMP. *Fuel* **2018**, *212*, 12–18. [CrossRef]
30. Yin, J.; Lin, X.; Wang, C.; Dai, J.; Wang, Y.; Xu, Z. Identification of the transformation features of heteroatomic compounds in a low rank coal by combining thermal extraction and various analytical approaches. *Fuel* **2020**, *270*, 117480. [CrossRef]
31. Mahat, R.K.; Rodgers, W.; Basile, F. Microwave Radiation Heating in Pressurized Vessels for the Rapid Extraction of Coal Samples for Broad Spectrum GC–MS Analysis. *Energ. Fuel* **2014**, *28*, 6326–6335. [CrossRef]
32. Yoshida, T.; Takanohashi, T.; Sakanishi, K.; Saito, I.; Fujita, M.; Mashimo, K. The effect of extraction condition on "Hyper Coal" production (1) under room-temperature filtration. *Fuel* **2002**, *81*, 1463–1469. [CrossRef]
33. Liu, L.; Kumar, S.; Wang, Z.; He, Y.; Liu, J.; Cen, K. Catalytic effect of metal chlorides on coal pyrolysis and gasification part I. Combined TG-FTIR study for coal pyrolysis. *Thermochim. Acta* **2017**, *655*, 331–336. [CrossRef]
34. Iino, M.; Takanohashi, T.; Ohsuga, H.; Toda, K. Extraction of coals with CS2-N-methyl-2-pyrrolidinone mixed solvent at room temperature: Effect of coal rank and synergism of the mixed solvent. *Fuel* **1988**, *67*, 1639–1647. [CrossRef]
35. Bao, Y.; Hu, Y.; Wang, W.; Guo, C.; Wang, G. Accumulation model and geochemistry characteristics of oil occurring from Jurassic coal measures in the Huangling mining area of the Ordos Basin, China. *Front. Earth Sci.-Prc.* **2023**, *17*, 158–169. [CrossRef]
36. *GB/T 1314-2007*; Gray-King Assay of Coal. Standardization Administration of China: Beijing, China, 2007. (In Chinese)
37. Bao, Y.; Li, Z.; Meng, J.; Chen, X.; Liu, X. Reformation of coal reservoirs by microorganisms and its significance in CBM exploitation. *Fuel* **2024**, *360*, 130642. [CrossRef]
38. Painter, P.C.; Snyder, R.W.; Starsinic, M.; Coleman, M.M.; Kuehn, D.W.; Davis, A. Concerning the application of FT-IR to the study of coal: A critical assessment of band assignments and the application of spectral analysis programs. *Appl. Spectrosc.* **1981**, *35*, 475–485. [CrossRef]
39. Ibarra, J.; Muñoz, E.; Moliner, R. FTIR study of the evolution of coal structure during the coalification process. *Org. Geochem.* **1996**, *24*, 725–735. [CrossRef]
40. Supaluknari, S.; Larkins, F.P.; Redlich, P.; Jackson, W.R. An FTIR study of Australian coals: Characterization of oxygen functional groups. *Fuel Process. Technol.* **1988**, *19*, 123–140. [CrossRef]
41. Mastalerz, M.; Bustin, R.M. Electron microprobe and micro-FTIR analyses applied to maceral chemistry. *Int. J. Coal Geol.* **1993**, *24*, 333–345. [CrossRef]
42. Thomas, N.; Liliedahl, T.; Krister, S. Metallic iron as a tar breakdown catalyst related to atmospheric, fluidised bed gasification of biomass. *Fuel* **2006**, *85*, 689–694. [CrossRef]
43. Taralas, G.; Kontominas, M.G. Kinetic modelling of VOC catalytic steam pyrolysis for tar abatement phenomena in gasification/pyrolysis technologies. *Fuel* **2004**, *83*, 1235–1245. [CrossRef]

44. He, X.; Liu, X.; Nie, B.; Song, D. FTIR and Raman spectroscopy characterization of functional groups in various rank coals. *Fuel* **2017**, *206*, 555–563. [CrossRef]
45. Li, D.; Bao, Y.; Wang, Y.; An, C.; Chang, J. Multiple-experimental investigation on the physicochemical structures alternation during coal biogasification. *Fuel* **2023**, *339*, 127433. [CrossRef]